SIMULATION OF SHOCK-INITIATED IGNITION

Melguizo-Gavilanes, J., Rezaeyan, N. and Bauwens, L.
University of Calgary, Department of Mechanical and Manufacturing Engineering,
2500 University Dr. NW, Calgary, AB T2N 1N4, Canada, jmelguiz@ucalgary.ca

ABSTRACT

The scenario of detonative ignition in shocked mixture is quite relevant to hydrogen safety, because hydrogen is prone to detonation and shock reflections may result in deflagration to detonation transition. However, even in one dimension, simulation of ignition between a contact surface or a flame and a shock moving into a combustible mixture is difficult because of the mathematical singularity present in the initial condition. Indeed, initially, as the shock starts moving into reactive mixture, the region filled with reactive mixture has zero thickness. Thus, on a fixed grid, the number of grid points between the shock and the contact surface increases as the shock moves away from the latter. Staircasing (the resulting plots will be functions composed of sets of equally spaced jumps of equal length) takes place and it will be amplified by the chemistry which is very sensitive to temperature, leading to unreliable results. In the current work, the formulation is transformed, using time and length over time as the independent variables. This frame of reference corresponds to the self-similar formulation in which the non-reactive problem remains stationary. Thus the initial singularity is removed and the initial process is well-resolved. The numerical solution uses an Essentially Non-Oscillatory algorithm, which is adequate not only for the early part of the process, but also for the latter part, when chemistry leads to appearance of a shock and eventually a detonation wave is formed.

NOMENCLATURE

E	activation energy
e	internal energy
K	rate multiplier
p	pressure
Q	total heat release
T	temperature
t	time
u	velocity
x	longitudinal coordinate
λ	mass fraction
η	$=x/t$
γ	ratio of specific heats
ρ	density
M	Mach Number
Subscripts	
s	postshock state
o	preshock state

1 INTRODUCTION

The risk of hydrogen detonation, especially in enclosed environments such as tunnels and garages, remains of concern from the standpoint of safety of hydrogen as an automotive energy carrier. Shock reflections heating reactive mixture may play an important role in the deflagration to detonation transition

(DDT) process. In shocked mixture, an induction time gradient exists, associated with the Zel'dovich spontaneous flame model [1]. Theoretical models in the Newtonian limit γ close to unity are able to account for the interplay between gas dynamics and chemistry [2, 3, 4]. However, that approximation does not resolve weak shock cases, behind which the Mach number is greater than $1/\sqrt{\gamma}$, so that chemistry and heat release result in a temperature decrease. For the general case, there does not appear to be alternatives to numerical simulation.

The initial value problem being solved will represent either a shock that reflected from a boundary, or a shock that came from inert (or burnt) mixture, and propagates into fresh reactive mixture, at different temperatures. The latter case represents a shock crossing over a flame, neglecting the flame propagation speed, which is typically small compared with the shock speed. In all these scenarios, the initial extent of reactive mixture between the shock and the contact surface separating fresh and wall/warm reacted mixture/inert mixture is initially zero. The shock will then move into fresh mixture, and, on a regular spatial grid, there will initially be one, then two, then a few grid points in the region of interest. This may lead to staircasing and ultimately amplification by chemistry of initial numerical artifacts.

An interesting approach avoiding that issue was used by Short & Dold [5], in which the original problem formulation using space x and time t as the independent variables is converted into a problem in $\eta = x/t$ and t. In the absence of chemistry, the problem would be self-similar in x/t. The initial domain becomes finite and the solution is then well resolved especially at early times. In contrast with Short & Dold [5], here the transformed problem is solved using a second order ENO algorithm, which is suited to handle not only hot spot formation but the entire process, including rapid growth of the hot spot, shock formation and the appearance of a detonation wave. Results for single step kinetics are in good agreement with a recent study performed by Sharpe & Short [6] on a fixed grid, but in which grid refinement was used to improve the resolution in the neighborhood of the hot spot.

The physical model includes the reactive Euler's equations. In the transformed independent variable η, initially the leading shock is located at a value η_s equal to the the opposite of the speed at which the shock is moving away from the contact surface, located at $\eta_{cs} = 0$. Thus the solution domain goes from a negative value of η somewhat smaller than η_s to a positive value somewhat larger than the speed of sound in the burnt (or non-reactive) mixture behind the contact surface. In this way, the full resolution is available in the region between shock and contact surface already from the initial time, overcoming the difficulty due to non-existence of an initial physical domain, when solving this problem on a normal spatial domain. Resulting initial conditions are shown below in the physical model.

Below, the transformed problem is presented, then the numerical solution is briefly described. Validation results for single step Arrhenius kinetics are presented and compared with results from the literature.

2 PHYSICAL MODEL

The problem is described by the reactive Euler's equations. Taking the conditions between the contact surface and the shock as a reference, pressure, density and temperature were scaled by their postshock values, velocity by the postshock speed of sound, heat release, internal energy and activation energy by the postshock speed of sound squared, and length and time in a ratio equal to the post shock speed of sound. For single step Arrhenius kinetics, the dimensionless conservation laws written in conservative form are:

$$\frac{\partial \rho}{\partial t} + \frac{\partial (\rho u)}{\partial x} = 0 \tag{1}$$

$$\frac{\partial (\rho u)}{\partial t} + \frac{\partial}{\partial x}(\rho u^2 + p) = 0 \tag{2}$$

$$\frac{\partial(\rho e)}{\partial t} + \frac{\partial}{\partial x}[u(\rho e + p)] = 0 \tag{3}$$

$$\frac{\partial(\rho\lambda)}{\partial t} + \frac{\partial(\rho u\lambda)}{\partial x} = \rho K(1-\lambda)exp(-E/T) \tag{4}$$

Where ρ is the density, u is velocity, p is pressure, e is the internal energy, λ is the mass fraction of the product, K is the reaction rate, e is the activation energy and T is the temperature. The time scale, which has so far been left undefined, can be set such that the dimensionless reaction rate $K = 1$. Finally, temperature and internal energy are related to pressure, density, mass fraction and velocity by

$$p = \rho T, \qquad e = \frac{p}{(\gamma-1)\rho} + \frac{u^2}{2} - Q\lambda \tag{5}$$

To deal with the initial singularity, whereby the initial domain of interest has zero length, a transformed frame of reference is introduced, replacing x and t as the independent variables by $\eta = x/t$ and t. In the transformed formulation, using the chain rule, the dimensionless conservation laws become:

$$\frac{\partial(t\rho)}{\partial t} + \frac{\partial}{\partial \eta}(\rho u - \eta\rho) = 0 \tag{6}$$

$$\frac{\partial(t\rho u)}{\partial t} + \frac{\partial}{\partial \eta}(\rho u^2 + p - \eta\rho u) = 0 \tag{7}$$

$$\frac{\partial(t\rho e)}{\partial t} + \frac{\partial}{\partial \eta}[u(\rho e + p) - \eta\rho e] = 0 \tag{8}$$

$$\frac{\partial(t\rho\lambda)}{\partial t} + \frac{\partial}{\partial \eta}(\rho u\lambda - \eta\rho\lambda) = t\rho(1-\lambda)exp(-E/T) \tag{9}$$

The solution domain goes from a negative fixed value of η on the left, selected such that it is not reached by the shock or detonation wave at the end of the computation, to a positive value somewhat larger than the speed of sound in the inert mixture on the right. Boundary conditions include a supersonic inflow of unburnt reactive mixture ($\lambda = 0$) on the left, and a radiation condition on the right.

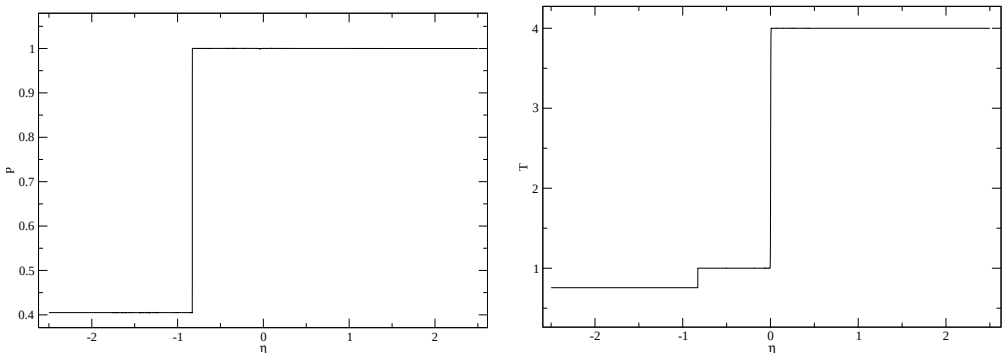

Figure 1: Initial conditions t = 0. Left: Pressure profile. Right: Temperature profile.

Initial conditions are shown in Figure 1, which shows the plots for pressure and temperature at t=0. They correspond to the solution to the non-reactive Riemann problem at $x = 0$. The frame of reference is set

such that initially the fluid behind the shock is at rest. Data for $x < 0$ correspond to the supersonic left boundary conditions. The contact surface separates unburnt shocked fluid from burnt or non-reactive fluid ($\lambda = 1$) initially in the positive x region, with the desired temperatures on both sides of the contact surface, located at $\eta = 0$. (The expansion wave moving right is immaterial to the problem at hand.) The dimensionless state ahead of the shock is determined as a function of the shock Mach number using the Rankine-Hugoniot equations which for the current formulation yield:

$$\rho_o = \frac{(\gamma+1)}{(\gamma-1)+2/M_s^2} \tag{10}$$

$$p_o = \frac{2\gamma M_s^2 - (\gamma-1)}{(\gamma+1)} \tag{11}$$

$$u_o = \frac{\sqrt{\gamma} M_s (1-\rho_o)}{\rho_o} \tag{12}$$

3 NUMERICAL SIMULATION

The problem described above is solved numerically using a second order accurate ENO scheme. The code used originated in [7], but that code has since been significantly modified and it has been parallelized using MPI (Message Passing Interface). The code is well-validated. It has been used successfully in a number of studies, mostly of the structure of multidimensional detonation waves [8, 9] but also of realistic hydrogen accident scenarios [10] and in a one-dimensional accelerating flame problem [11].

Solving the problem above, in the transformed frame of reference, entailed a proper derivation of he CFL condition formulated in the transformed frame of reference η and t.

The numerical resolution domain is readily determined from the actual domain. In η, the solution domain goes from a negative value of η slightly smaller than η_s (the initial speed of the leading shock) to a positive value somewhat larger than the local speed of sound behind the contact surface. This guarantees that the leading shock will never reach the left boundary. Likewise, since the right boundary is placed at a value of η greater than the speed of sound behind the contact surface, acoustic waves originating from the reaction zone and going across the contact surface will never reach the right boundary.

4 RESULTS

For validation purposes, the solution was obtained for one of the cases presented in detail by Sharpe and Short [6]. A resolution study was performed, progressively doubling the number of grid points along η, from 6,400 to 102,400, at which point no significant difference could longer be seen in the results.

The results below, obtained using a resolution of 51,200 grid points, are calculated for $Q = 4$, $E = 15$, $\gamma = 1.4$ and a shock Mach number $M_o = 1.5$. The density behind the contact surface was initially $\rho = 0.25$. Figures 2 and 3 show the evolution of pressure and temperature during the early stages of formation of the hot spot, very close to the contact surface, and its subsequent rapid growth. Figure 4 shows the reaction progress variable, during the induction phase (defined as the time that it takes for half of the fuel to be consumed). Figure 5 shows the subsequent evolution of the hot spot, still before the pressure waves steepen into shock waves. Figure 6 shows the temperature evolution for the same times as in Figure 5. Figure 7 and 8 show pressure and temperature respectively when transition into a detonation wave takes place, which eventually reaches the leading shock. Figure 9 shows the profiles for the reaction progress variables λ from the birth of the secondary shock to its transition into a detonation wave.

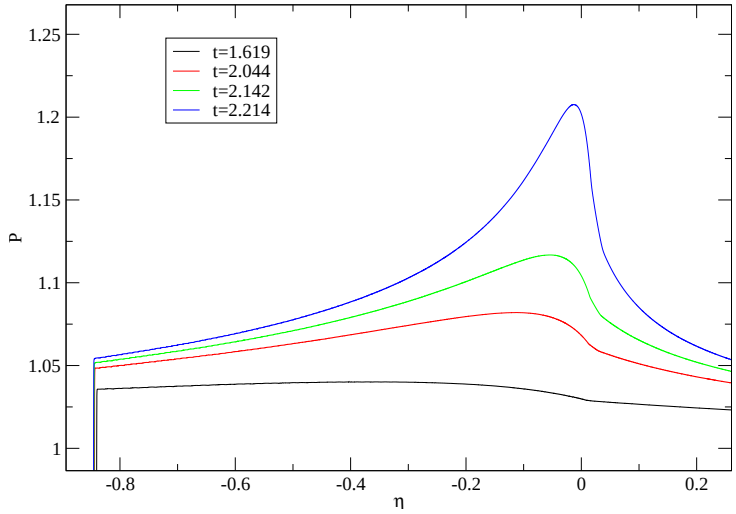

Figure 2: Pressure profiles for $Q = 4$, $\gamma = 1.4$, $E = 15$, at times $t = 1.619$, 2.044, 2.142 and 2.214. Early times: hot spot formation.

Figure 2 shows the pressure evolution during the early phase of hot spot formation. At t=1.619, the pressure maximum is located at some distance away from the contact surface. As time goes on, this pressure maximum moves closer to the contact surface, as the chemical reaction accelerates in the hot spot. The pressure maximum is located closest to the contact surface when t=2.214, which is the time of the last (highest) pressure profile plot in Figure 2.

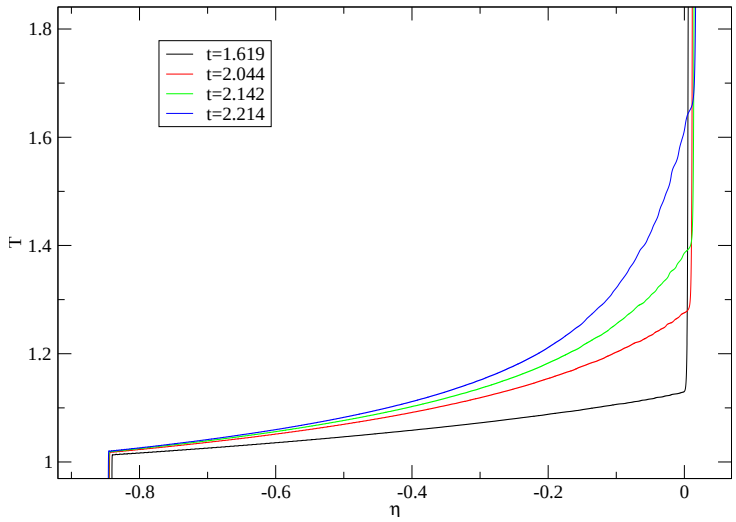

Figure 3: Temperature profiles $Q = 4$, $\gamma = 1.4$, $E = 15$, at times $t = 1.619$, 2.044, 2.142 and 2.214. Early times: hot spot formation.

Figure 3 shows the evolution of the temperature profiles during the same time period as in Figure 2. During this initial phase, temperature increases monotonically in space from the shock to the contact surface, which is consistent with the time period since local mixture was shocked. One also can see that the contact surface is being pushed toward the right due to the thermal expansion induced by chemistry. The temperature maximum remains located at the contact surface during this phase.

Figure 4 shows the evolution of the reaction progress variable (or combustion product mass fraction)

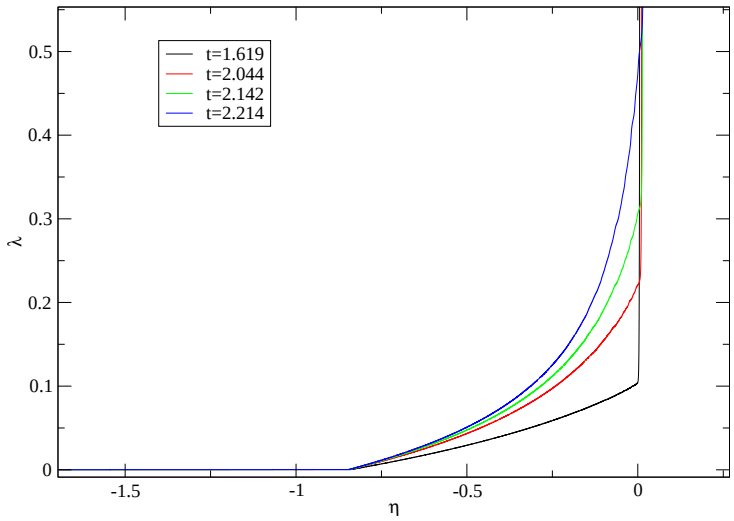

Figure 4: Mass fraction profiles $Q = 4$, $\gamma = 1.4$, $E = 15$, at times $t = 1.619$, 2.044, 2.142 and 2.214. Early times: hot spot formation.

during the induction stage, which goes from $1.619 < t < 2.214$. The mass fraction profiles behave similarly to the temperature profiles shown in Figure 3. During this time interval, mass fraction increases monotonically in space from the shock to the contact surface. Fresh mixture, characterized by $\lambda = 0$, is delivered by the shock and more of it becomes consumed at locations closer to the contact surface. The maximum value of the reaction progress variable in this plot is 0.5, which precisely indicates the end of the induction stage as half of the fuel has been consumed up to this point, close to the contact surface. Again, the figure shows contact surface being pushed toward the right due to thermal expansion in the region between shock and contact surface, where chemistry takes place.

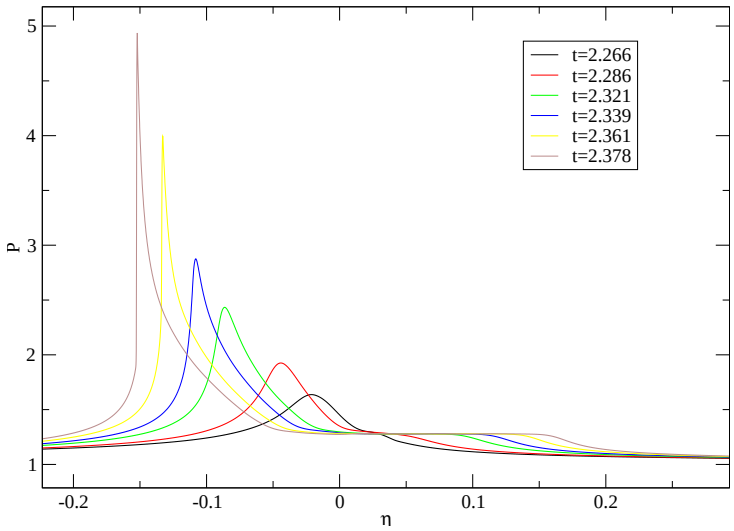

Figure 5: Pressure profiles for $Q = 4$, $\gamma = 1.4$, $E = 15$, at times $t = 2.266$, 2.286, 2.321, 2.339, 2.361 and 2.378

Figures 5 and 6 show the evolution of pressure and temperature profiles respectively, at later times. These were plotted for a larger domain on the right side, including values of $\eta > 0$, showing also how the variables evolve behind the contact surface. In both Figures 5 and 6, a pressure wave can be observed that moves towards the right into the burnt (or non-reactive) portion of the computational domain, beyond

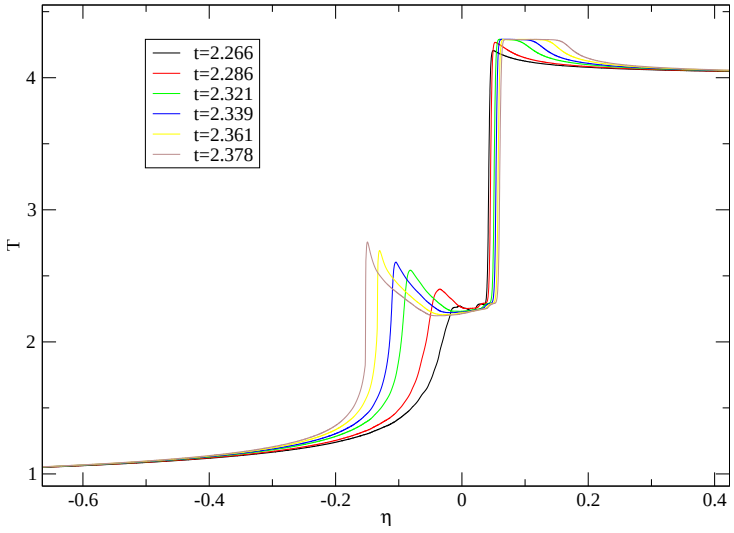

Figure 6: Temperature profiles for $Q = 4$, $\gamma = 1.4$, $E = 15$, at times $t = 2.266$, 2.286, 2.321, 2.339, 2.361 and 2.378

the contact surface, steepening up somewhat. Both pressure and temperature increase behind the contact surface, due to the compression resulting from thermal expansion produced by the chemical reaction behind the shock. Both pressure and temperature appear to reach a fixed maximum value. As this wave steepens further, it will eventually form a shock, known as a retonation wave. In contrast, in the absence of chemistry, the temperature behind the contact surface would have remained unchanged.

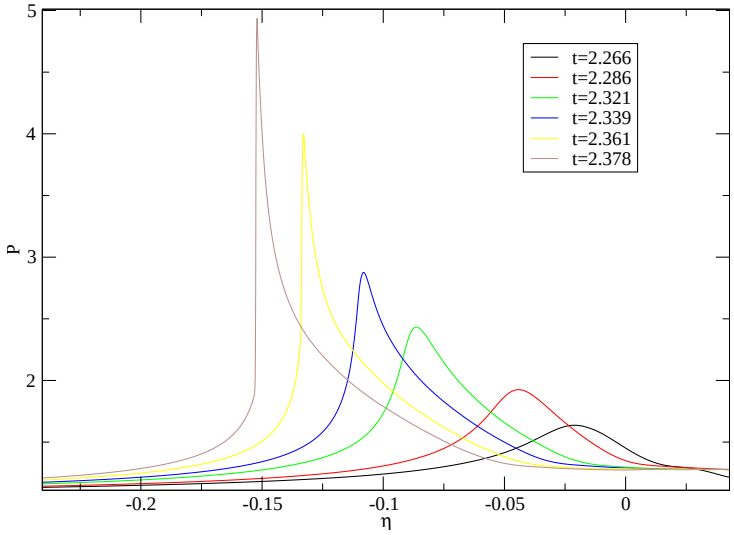

Figure 7: Pressure profiles for $Q = 4$, $\gamma = 1.4$, $E = 15.$, at times $t = 2.266$, 2.286, 2.321, 2.339, 2.361 and 2.378. Later times: appearance of a detonation wave.

On the left, the evolution of the hot spot is shown in more detail in Figures 7 and 8, which show the pressure and temperature profiles while the hot spot further grows, and eventually transition into a detonation wave occurs. In Figure 7, the peak in pressure, which had previously been moving right now moves left, towards the leading shock and away from the contact surface. In Figure 8, in temperature, which initially, as shown in Figure 3, had been monotonically increasing toward and up to the contact surface, an internal temperature maximum now appears at $t = 2.266$ and moves left, away from the

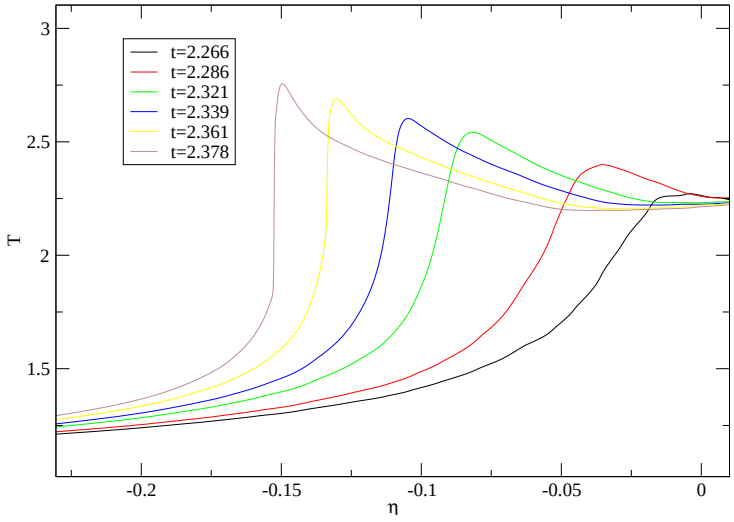

Figure 8: Temperature profiles for $Q = 4$, $\gamma = 1.4$, $E = 15.$, at times $t = 2.266$, 2.286, 2.321, 2.339, 2.361 and 2.378. Later times: appearance of a detonation wave.

contact surface. As time evolves, the peak in temperature continues moving away from the contact surface, catching up and eventually merging with the pressure peak. Profiles at later times show the pressure wave steepening into a new shock wave distinct from the leading shock hence appearance of a detonation wave, that moves toward and will eventually merge with the leading shock. (The merger occurs at a later times and it is thus not shown on the figures.)

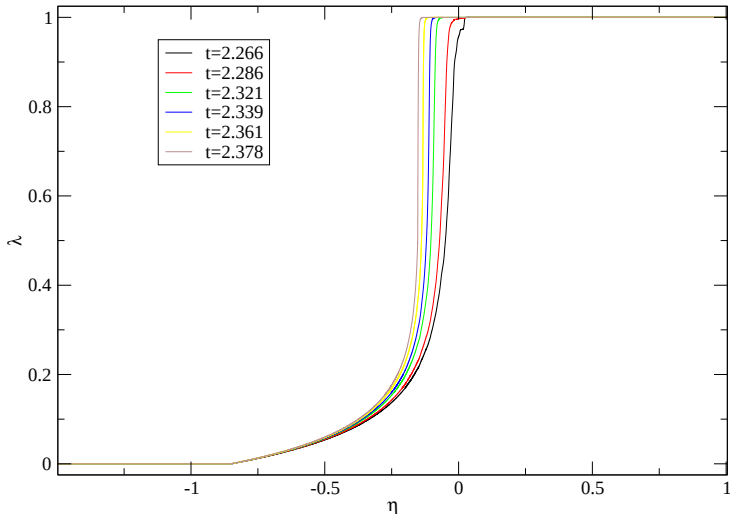

Figure 9: Mass fraction profiles for $Q = 4$, $\gamma = 1.4$, $E = 15.$, at times $t = 2.266$, 2.286, 2.321, 2.339, 2.361 and 2.378. Later times: appearance of a detonation wave.

As it moves toward the leading shock, this new detonation wave encounters mixture that is already partially burnt, but progressively less so. Thus the heat release available increases, which explains why this wave continues strengthening as the peak pressure and temperature continue growing. When it encounters the leading shock, a reflection takes place. A somewhat weaker detonation continues propagating into the colder mixture coming from left, while an expansion wave moves back toward the right.

In Figure 9, for $t = 2.266$, which is the time at which the peak in temperature starts to move off the contact surface towards the leading shock, the reactant is largely but not fully consumed at the contact surface, indeed $\lambda = 0.95$ at this point. For the rest of the times shown, once the secondary shock gains more strength, the reactant is consumed almost instateneously consistent with the one-step reaction model with Arrhenius kinetics used to model the chemistry in our simulation.

These results are consistent with Sharpe et al. [6], validating the current formulation and its implementation. Next, the code will be used for a more thorough exploration of the parameter space, and also, for more realistic chemical kinetics, consistent with hydrogen-air chemistry.

5 CONCLUSION

A simulation of ignition between a contact surface and a shock was performed in one dimension, using a transformed coordinate system that overcomes the inherent initial singularity present in the original physical problem formulation. In the new coordinate system, additional terms appear in the governing equations. As a result, an appropriate implementation of the ENO scheme entailed a different CFL condition. Results show the complete chain of events that takes place during shock ignition, from slow formation and rapid growth of the hot spot to the birth of a secondary shock and its transition into a detonation wave. Small pressure waves moving to the right behind the contact surface were also captured by our calculations. During the induction phase the pressure peak first appeared somewhere in the region between the shock and the contact surface and started to move closer to the latter, whereas for the same time interval the temperature peak was always located at the contact surface. For later times the pressure and temperature peaks started to move toward the leading shock, with the pressure peak located slightly ahead of its temperature counterpart. Eventually both of the peaks were located at the same value of η and the steepening pressure wave moving left turned into a shock wave thus the entire structure became a detonation wave that continued steepening as it moved into fresher partially burnt mixture. These simulations confirmed that indeed ignition takes place a small distance ahead of the contact surface. These preliminary results are in close agreement with those obtained by Sharpe et al. [6]. With single step kinetics, it appears that chemistry behind the shock always leads to appearance of a detonation wave. Next, however, the current approach will be used to compare the current results with different kinetic models such simplified chain-branching schemes [8, 9], which are expected to result in different conclusions potentially with different regimes depending upon the location of the post-shock mixture in the chain-branching explosion diagram.

ACKNOWLEDGMENTS

Work supported by the Natural Science and Engineering Research Council of Canada, The AUTO21 Network of Centres of Excellence and Natural Resources Canada. The University of Calgary is a member of the HySafe Network of Excellence

REFERENCES

[1] Zel'dovich, Ya. B., Librovich, V.B., Makhviladze, G.M. and Sivashinsky, G.I., On the Development of Detonation in a Non-Uniformly Preheated Gas, *Astronautica Acta*, **15**, 1970, pp. 313-321.

[2] Blythe, P.A. & Crighton, D.G., Shock-generated ignition: the induction zone, *Proceedings of the Royal Society of London A*, **426**, 1989, pp. 189-209.

[3] Bauwens, L., Ignition between a Shock and a Contact Surface: Influence of the Downstream Temperature, *Proceedings of the Combustion Institute*, **28**, 2000, pp. 653-661.

[4] Bauwens, L. and Liang, Z., Shock Formation Ahead of Hot Spots, *Proceedings of the Combustion Institute*, **29**, 2003, pp. 2795-2802.

[5] Short, M., Dold, W., Unsteady Gasdynamic evolution of an induction domain between a contact surface and a shock wave. I: Thermal Runaway, *SIAM Journal of Applied Mathematics*, **56**, 1996, pp. 1295-1316.

[6] Sharpe, G.J., Short, M., Ignition of thermally sensitive explosives between a contact surface and a shock, *Phys. Fluids*, **19**, 2007, 126102.

[7] Xu S.J., Aslam T., Stewart, D.S., High resolution numerical simulation of ideal and non-ideal compressible reacting flows with embedded internal boundaries, *Combustion Theory and Modelling*, **1**, 1997, pp. 113-142.

[8] Liang, Z. and Bauwens, L., Cell Structure and Stability of Detonations with a Pressure Dependent Chain-Branching Reaction Rate Model, *Combustion Theory and Modelling*, **9**, No. 1, 2005, pp. 93-112.

[9] Bédard-Tremblay, L., Melguizo-Gavilanes, J. and Bauwens, L., Detonation Structure under Chain-Branching Kinetics with Small Initiation Rate, *Proceedings of the Combustion Institute*, **32**, 2009, pp. 2339-2347.

[10] Bédard-Tremblay, L., Fang, L., Melguizo-Gavilanes, J., Bauwens, L., Finstad, P.H.E., Cheng, Z. and Tchouvelev, A.V., Simulation of Detonation after an Accidental Hydrogen Release in Enclosed Environments, *International Journal of Hydrogen Energy*, 2009, doi:10.1016/j.ijhydene.2009.01.097.

[11] Bauwens, L., Bauwens, C.R.L. and Wierzba, I., Oscillating flames: multiple scale analysis, *Proceedings of the Royal Society of London A*, 2009, doi:10.1098/rspa.2008.0388.